

# Precision Ethylene/Vinyl Chloride Polymers via Condensation Polymerization

Emine Boz,<sup>†</sup> Alexander J. Nemeth,<sup>†</sup> Ion Ghiviriga,<sup>†</sup> Keesu Jeon,<sup>‡</sup> Rufina G. Alamo,<sup>‡</sup> and Kenneth B. Wagener<sup>\*,†</sup>

*The George and Josephine Butler Polymer Research Laboratory and Center for Macromolecular Science and Engineering, Department of Chemistry, University of Florida, Gainesville, Florida 32611-7200, and Department of Chemical and Biomedical Engineering, FAMU/FSU College of Engineering, Tallahassee, Florida 32310-6046*

*Received April 21, 2007; Revised Manuscript Received June 24, 2007*

**ABSTRACT:** A family of precision ethylene/vinyl chloride polymers synthesized via acyclic diene metathesis (ADMET) followed by exhaustive hydrogenation is described in which chlorine atoms are present on each and every ninth, 15th, and 21st carbons, respectively, in the series. Detailed <sup>1</sup>H NMR and <sup>13</sup>C NMR experiments are used to establish the precise nature of the polymers and assign absolutely the observed NMR signals to the corresponding atoms in the precise repeat unit. Thermal analysis via TGA and DSC is also presented. Decomposition behavior measured by TGA indicates a distinct mechanism for decomposition for these precise polymers relative to PVC and random EVC polymers, highlighted by an enhanced stability to thermal HCl loss induced by inhibition of the cooperative zipper mechanism for HCl found in PVC. A homopolymer-like crystallization and melting behavior is inferred from sharp DSC peaks, indicative of a precise polymer structure in which long chain segments, incorporating the halogens, build the core crystal, as opposed to the sequence selection mechanism that operates in random EVC polymers.

## Introduction

As the second largest volume plastic produced in industry,<sup>1</sup> poly(vinyl chloride) (PVC) continues to find a growing range of applications and is projected to have an increasing demand in the near future.<sup>2</sup> Common applications of PVC include pipes, siding, molding, windows, and flooring.<sup>3</sup> For many applications, the properties of PVC must be modified in order to increase performance and stability. While the addition of additives is the most common way to modify the characteristics of PVC for a specific application, the physical properties and stability are greatly affected by the primary structure of the PVC itself.<sup>4</sup> For example, the amount of syndiotactic segments in PVC has a strong effect on the melting point and overall crystallinity of the polymer and the content of defects, such as branching, head-to-head linkages, and unsaturated sites plays a major role in determining the stability of PVC to the “zipper” mechanism responsible for its degradation at elevated temperatures. The occurrence of defects and the lack of control over primary structure is the consequence of the free-radical initiated methods, which are used in the synthesis of nearly all PVCs produced.<sup>5</sup> On the basis of this and the ubiquitous use of additives to modify properties in PVC, detailed information about the effect of primary structure on materials properties is often not pursued. However, vinyl chloride copolymers are used as a means to access a variety of new property sets and to combine the attractive properties of PVC with other polymers, while minimizing the weaknesses of PVC.<sup>6</sup>

Ethylene–vinyl chloride (EVC) copolymers are an attractive class of polymers, which are pursued as a means of capitalizing

on the strengths of PVC and polyethylene (PE). Here, judicious compositional control is a route to developing a series of polymers with accurately controlled properties as determined by the composition of the polymer itself. However, on the basis of the methods by which these EVC polymers are usually synthesized, little primary structure control is achieved, and the more-or-less random structures give little information about how chlorine content and sequence distribution directly affect the materials properties of the polymers. There are three common methods for the preparation of EVC polymers: copolymerization of ethylene and vinyl chloride using free radical<sup>7–9</sup> or Ziegler–Natta techniques,<sup>10,11</sup> reductive dechlorination of PVC,<sup>12–14</sup> and chlorination of polyethylene.<sup>15–18</sup> In the direct free radical copolymerization of vinyl chloride and ethylene, it is difficult to control the content of the two monomer units over the full range of compositions.<sup>19</sup> Further, the free radical nature of the polymerization leads to poorly defined structures with high defect contents. Direct copolymerization of vinyl chloride and ethylene using Ziegler–Natta or metallocene catalysts is also problematic based on the occurrence of side reactions with the activated chlorine atom on the monomer and the alkylaluminum cocatalyst as well as the tendency of the vinyl chloride monomer to undergo  $\beta$ -halo elimination after insertion into the metal–alkyl bond.<sup>10,11</sup> In the case of the reductive dechlorination of PVC, while the ability to generate a family of EVC polymers with varying Cl contents and with identical chain lengths from a single PVC sample is a strong point for a model,<sup>20</sup> this class still suffers from defects present in the parent PVC.<sup>21</sup>

The most common method used for synthesizing EVC polymers is the chlorination of PE either under homogeneous or heterogeneous conditions. In homogeneous, or solution-based, techniques chlorine is distributed randomly throughout the polymer.<sup>18</sup> At low chlorine contents, the probability of chlorine substitution on a CHCl unit or neighboring unit is very small based on the bulky Cl atom, resulting in a random spatial distribution of Cl atoms along the backbone. At higher chlorine

\* Corresponding author. E-mail: wagener@chem.ufl.edu.

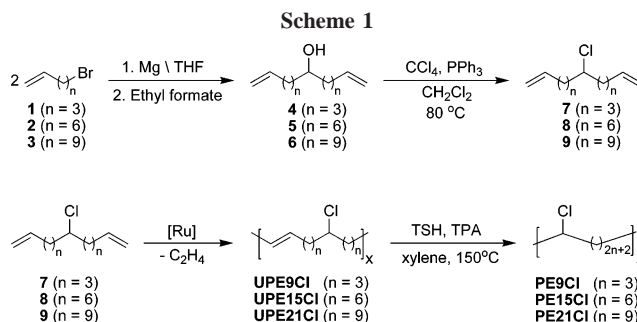
<sup>†</sup> The George and Josephine Butler Polymer Research Laboratory and Center for Macromolecular Science and Engineering, Department of Chemistry, University of Florida.

<sup>‡</sup> Department of Chemical and Biomedical Engineering, FAMU/FSU College of Engineering.

contents, however, geminal chlorination and vicinal chlorination becomes more commonplace.<sup>22–24</sup> In heterogeneous methods such as suspension, or solid state, the main drawback here is the blocky nature of the formed polymers based on the tendency for chlorination to occur in the amorphous regions of the polymer and at the edge of the crystalline domains.<sup>17,25</sup> Considering the above methods for attaining EVC polymers, it is clear that control over chlorine content can be achieved in each of these methods, but control over sequence distribution cannot be attained. Therefore, even though the properties of EVC polymers with different chlorine contents are known to vary, deriving exact relationships between primary structure and physical properties is unattainable because a precise distribution of comonomer units between crystalline and amorphous domains has yet to be determined.<sup>26</sup>

Despite the lack of a precise model for understanding the variation in the properties of EVC polymers, there is great practical interest in these materials.<sup>25</sup> Specifically, the introduction of ethylene units into a PVC chain will serve the role of an internal plasticizer, which can give many advantages over the introduction of an external plasticizer and lead to a new range of materials properties from a single component material.<sup>19,27</sup> From a more fundamental standpoint, this class of polymers is also of great interest for developing a precise understanding of the relationship between molecular structure and physical properties in semicrystalline polymers in general, where EVC polymers could serve as an all-purpose model for this class of polymers.<sup>25</sup> As described above, however, no specific catalyst system has been developed to effectively copolymerize ethylene and vinyl chloride, leading to the necessity to look toward model EVC polymers to establish the fundamental significance of this class of polymer. Such a focus on model polymers will not only help to derive structure property relationships but also shift focus to the development of effective catalysts for the synthesis of EVC copolymers.<sup>28</sup> It is difficult however to find suitable model systems that will allow for the development of precise structure property relationships<sup>29</sup> and will not be limited by the quality of the synthetic or preparative method.

Recently, olefin metathesis chemistry combined with post-polymerization hydrogenation has emerged as an attractive route for synthesizing polyolefins bearing a variety of substituents.<sup>30</sup> For EVC polymers, ring opening metathesis polymerization (ROMP) has been employed to make a series of polymers with varying chlorine contents.<sup>31</sup> The absence of defects in polymers produced by ROMP leads to materials with well-defined primary structures and chlorine contents that are tuned by controlling the ratio between chlorinated and non-chlorinated monomers. The sequence distribution is nonetheless still random. Alternatively, acyclic diene metathesis polymerization (ADMET) has been used to achieve an EVC polymer with both precisely controlled chlorine content and sequence distribution,<sup>32</sup> here such a level of control allows one to derive precise relationships between polymer primary structure and physical properties in EVC polymers. Further, ADMET allows the investigation of a much greater range of polymers with precisely distributed chlorine atoms, as the linear  $\alpha$ - $\omega$  dienes used in ADMET are free of the structural constraints required for monomers used in ROMP. We present here the full characterization of a new expanded family of precise EVC polymers in which a range of precise chlorine contents and sequence distributions are examined in order to generate structure–property relationships useful for developing a deeper understanding of the importance of primary structure control in EVC polymers.



## Results and Discussion

**Monomer and Polymer Synthesis.** Synthesis of the necessary chlorinated  $\alpha$ - $\omega$  diene monomers is illustrated in Scheme 1. The alcohol precursors (**4**–**6**) were prepared as described earlier.<sup>33</sup> Conversion of the alcohols to the corresponding chlorine monomers (**7**–**9**) by reaction with carbon tetrachloride and triphenylphosphine preceded bulk polymerization with Grubbs' first generation ruthenium catalyst to yield the unsaturated ADMET polymer UPEXCl. The nomenclature acronym used herein is UPEXCl, where U indicates unsaturation and PEXCl indicates a polyethylene backbone with a chlorine substituent on every Xth carbon, where X = 9, 15, 21. Exhaustive hydrogenation by diimide reduction<sup>34</sup> gave clean conversion to the fully saturated polymers **PE9Cl**, **PE15Cl**, and **PE21Cl**. Polymer molecular weights are shown in Table 1 and vary between 31 000 and 51 000 g/mol.

**Primary Structure Characterization.** The primary structure of these well-defined UPEXCl and PEXCl polymers was established using a combination of <sup>1</sup>H NMR, <sup>13</sup>C NMR, TGA (thermogravimetric analysis), IR spectroscopy, and elemental analysis. Figure 1 shows the <sup>1</sup>H NMR and <sup>13</sup>C NMR spectra for a typical conversion of a symmetrical chlorine containing  $\alpha$ - $\omega$  diene monomer **7**, 6-chloroundeca-1,10-diene, to its unsaturated ADMET polymer **UPE9Cl**, and then to its precisely substituted saturated polymer analogue with a chlorine atom on each and every ninth carbon **PE9Cl**.

Parts a and d of Figure 1 illustrate the <sup>1</sup>H NMR and <sup>13</sup>C NMR spectra for the monomer **7** showing the assigned protons and carbons 1 through 6 in (5.0, 5.8, 2.1, 1.5, 1.7, 3.9 ppm) <sup>1</sup>H NMR data and in (115.1, 138.6, 33.4, 25.9, 38.1, 64.0 ppm) <sup>13</sup>C NMR data, respectively. Parts b and e of Figure 1 illustrate the <sup>1</sup>H NMR and <sup>13</sup>C NMR spectra for the unsaturated ADMET polymer **UPE9Cl**. In the proton spectrum (Figure 1b) two triplets are observed in the region 5.34–5.40, corresponding to the *cis* and *trans* configurations of the double bond. The <sup>13</sup>C satellite of the major peak is a doublet of triplets, with a coupling constant of 17.5 Hz, therefore the major peak was assigned to *trans*. The *trans*:*cis* ratio determined from the carbon spectrum (Figure 1e) is 4:1. The peaks for the terminal vinyl moiety appeared at 4.99 (*CH*<sub>2</sub> *trans*), 4.93 (*CH*<sub>2</sub> *cis*), and 5.81 (*CH*). The degree of polymerization (DP) was determined by integration of these signals against the two triplets in the region 5.34–5.40, and the values are shown in Table 2. The proton signals for **UPE9Cl** were assigned from the DQCOSEY spectrum. The protons in positions 1 and 2 displayed different chemical shifts in the *trans* and *cis* moieties, being 0.03 ppm upfield and 0.03 ppm downfield in *cis* as compared to *trans*, in positions 1 and 2, correspondingly. The GHMBC spectrum revealed both the one-bond and the two- or three-bond couplings between protons and carbons, for both the *cis* and the *trans* moieties. The proton and carbon chemical shifts have been assigned based on these cross-peaks and are presented in Table 2, together with the *trans*:*cis* ratio.

Table 1. Molecular Weight and Thermal Data for Unsaturated (UPEXCl) and Saturated (PEXCl) Polymers

sample	$M_w \times 10^3$	$M_w/M_n$	$T_g$ (°C)	$T_m$ (°C)	$T_c$ (°C)	$\Delta H_m$ (J/g)	onset of decomposition (°C)	
							first stage <sup>e</sup>	second stage <sup>f</sup>
UPE9Cl	37 <sup>a</sup>	1.84	−63				292	385
UPE15Cl	40 <sup>a</sup>	1.81	−57	24	−6	27	320	413
UPE21Cl	67 <sup>a</sup>	1.84	−37	46	32	67	332	415
PVC	43	1.95	80				274	450
PE9Cl	49 <sup>a</sup>	1.78	−33	41	15	26.7	295	418
PE15Cl	51 <sup>a</sup>	1.75		63	54	87.4	301	420
PE21Cl	31 <sup>b</sup>	4.43		81	70	111.3	327	407
PE	16 <sup>c</sup>	1.60	−120 <sup>d</sup>	129	118	185.0	348	384

<sup>a</sup> GPC vs PS in THF. <sup>b</sup> GPC vs PE in DCB. <sup>c</sup> Reference 35. <sup>d</sup> Reference 36. <sup>e</sup> Recorded at first stage 10% total mass loss under nitrogen gas, 10 °C/min. <sup>f</sup> Recorded at second stage 10% total mass loss under nitrogen gas, 10 °C/min.

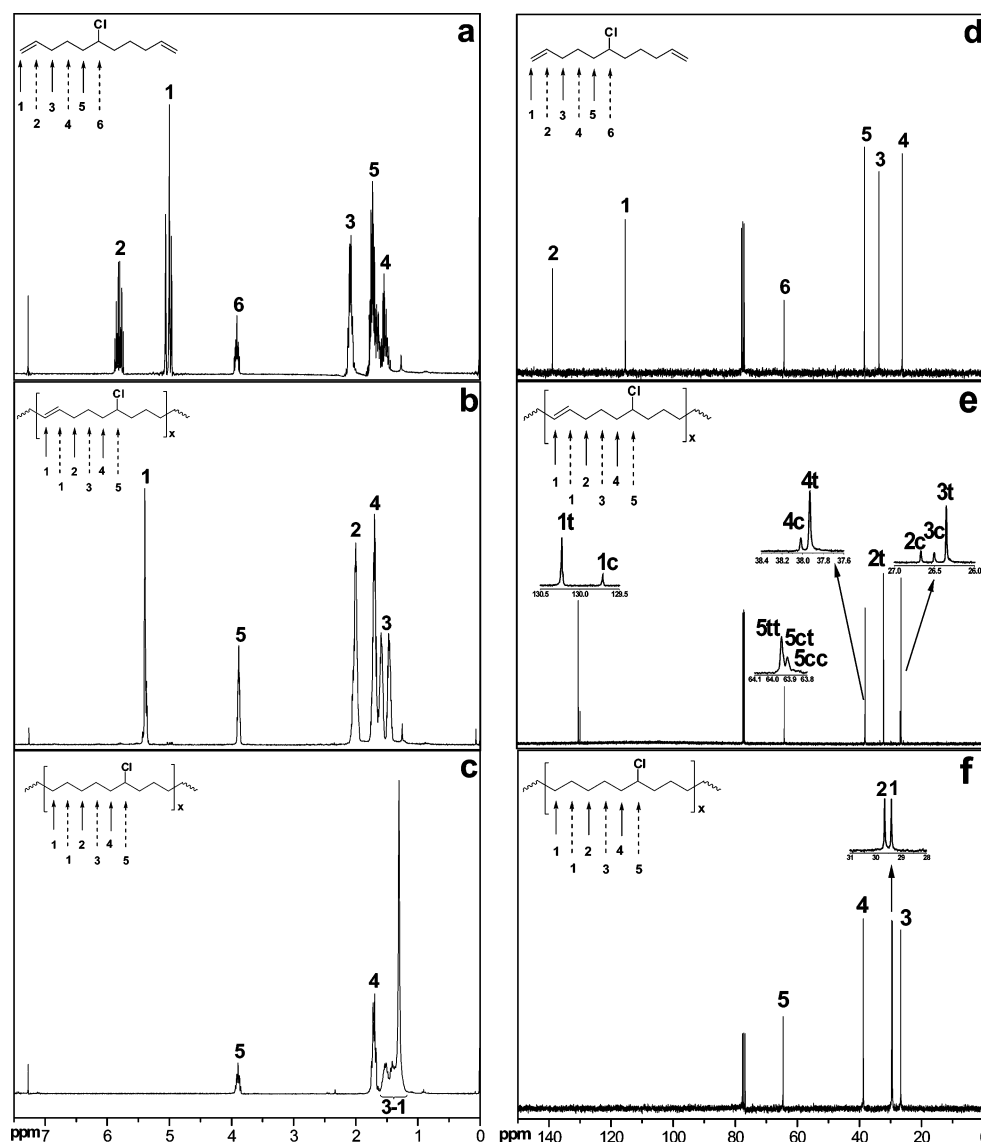


Figure 1.  $^1\text{H}$  NMR spectra for monomer **7** (a), UPE9Cl (b), PE9Cl (c) and  $^{13}\text{C}$  NMR spectra for monomer **7** (a), UPE9Cl (b), and PE9Cl (c).

The differences between the chemical shifts of a carbon atom in the *trans* and *cis* moieties,  $\Delta\delta_{\text{trans-cis}} = \delta_{\text{trans}} - \delta_{\text{cis}}$ , have been measured in a  $^{13}\text{C}$  spectrum acquired with a digital resolution of 0.9 ppb and are given, in ppb in Table 2.  $\Delta\delta_{\text{trans-cis}}$  are noticeable for carbons up to four bonds away from the double bond, and for an alkyl moiety free of the influence of other groups (double bonds or chlorine atoms must be some 7–10 bonds away) typical values in the order of distance, starting with the carbon of the double bond, are as follows: 465, 5339, −110, −137, and −37 ppb.

Further, in Figure 1c the  $^1\text{H}$  NMR for PE9Cl shows a methine proton ( $\alpha = 5$ ) at 3.9 ppm, and methylene protons ( $\beta = 4$ ) at 1.7 ppm and ( $\beta = 1-3$ ) at 1.2–1.6 ppm. The  $^{13}\text{C}$  NMR data exhibited in Figure 1f reveal that five  $\text{sp}^3$  carbon signals are present in this polymer, which contains a methine carbon ( $\alpha = 5$ , 64.6 ppm), and methylene carbons ( $\beta = 4$ , 38.8 ppm,  $\delta = 2$ , 29.6 ppm,  $\epsilon = 1$ , 29.4, and  $\gamma = 3$ , 26.7). The chemical shift ranges observed for polymer PE9Cl are in very good agreement with the values in the literature for the random ethylene/vinyl chloride copolymers.<sup>12,30,37,38</sup> In the random case, several

**Table 2.** Proton and Carbon Chemical Shifts (in ppm) and  $\Delta\delta_{trans-cis}$  (in ppb) for Polymers UPE9Cl, UPE15Cl, and UPE21Cl

compd	<i>trans:cis</i> DP	position	1	2	3	4	5	6	7	8	9	10	11
UPE9Cl	5.0	$\delta C$	130.20	32.00	26.40	37.90	64.00						
		$\Delta\delta_{trans-cis}$	514	5334	-148	-86	31						
		$\delta H$	5.40	1.99, 1.99	1.59, 1.46	1.70, 1.70	3.89						
UPE15Cl	4.4	$\delta C$	130.30	32.50	29.50	29.00	29.10	26.50	38.50	64.30			
		$\Delta\delta_{trans-cis}$	475	5387	-115	-136	-41	0	0	14			
		$\delta H$	5.38	1.97, 1.97	1.34, 1.34	1.27, 1.27	1.33, 1.30	1.51, 1.39	1.69, 1.69	3.88			
UPE21Cl	4.1	$\delta C$	130.30	32.60	29.70	29.20	29.49	29.56	29.52	29.20	26.50	38.50	64.30
		$\Delta\delta_{trans-cis}$	465	5399	-110	-137	-37	0	0	0	0	0	0
		$\delta H$	5.38	1.96, 1.96	1.33, 1.33	1.27, 1.27	1.27, 1.27	1.27, 1.27	1.27, 1.27	1.27, 1.27	1.51, 1.39	1.69, 1.69	3.88

different methine and other methylene chemical shifts are observed due to the random nature of the polymer structure. Obtaining only five different carbons for  $\sim 49\,000$  molecular weight polymers unequivocally confirms the precise structure of these polymers. These spectral data not only support the primary structure of the repeat unit but also suggest that no side reactions are detectable within the limitations of the NMR instrument. Elemental analysis results also show good agreement between theoretical and experimental values (see Experimental Section).

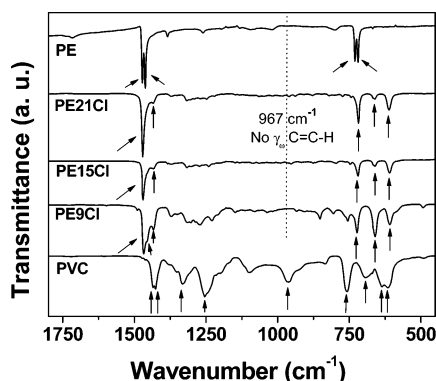
The olefin region in these NMR spectra also illustrates the conversion of monomer to unsaturated polymer with the disappearance of the terminal olefin at 5.0 and 5.8 ppm in the monomer and the subsequent growth of internal olefin resonance at 5.4 ppm in the unsaturated polymer **UPE9Cl**, a result consistent with the GPC results given in Table 1. Upon exhaustive hydrogenation, these olefin resonances completely disappear. The  $^{13}C$  NMR spectra support exhaustive hydrogenation as well; note that the  $sp^2$  resonances in the unsaturated polymer (*trans*, 130.2 ppm; *cis*, 129.7 ppm) completely disappear after hydrogenation giving **PE9Cl** (confirmed by IR). These spectra are typical for all the ADMET polyethylenes synthesized in the series, and they illustrate the degree of structure control that is possible. These conclusions are valid for the **UPE15Cl** and **UPE21Cl** polymers as well; the chemical shift values are given in Table 2 and in the Experimental Section. This detailed NMR study confirms the precise nature of the examined polymers and the degree of absolute control over primary structure afforded by ADMET polymerization followed by exhaustive hydrogenation.

The IR spectra in Figure 2 display characteristic information regarding the primary structure of the polymers, where the absence of a peak at  $967\text{ cm}^{-1}$  for all three EVC polymers indicates complete hydrogenation, based on the disappearance of the out-of plane olefin C–H wagging vibrational mode. The first spectral segment with characteristic information is the C–Cl stretching region between 600 and  $700\text{ cm}^{-1}$ . For PVC, three broad bands are observed centered at 615, 636, and  $693\text{ cm}^{-1}$

$\text{cm}^{-1}$ ,<sup>39</sup> where the “broadness” results from the contributions from a number of different conformations and configurations. For the EVC polymers, the resonances in the  $600\text{--}700\text{ cm}^{-1}$  region are significantly narrowed relative to PVC as the number of chlorines is reduced and number of  $\text{CH}_2$  sequences increased. The spectra then consist of two single narrow bands at  $660\text{--}661$  and  $609\text{--}611\text{ cm}^{-1}$ , which have been assigned to isolated *gauche*, and *trans* C–Cl stretching respectively.<sup>40</sup> Going from **PE9Cl** to the **PE21Cl** decreases the *gauche* to *trans* ratio as the number of  $\text{CH}_2$  units between Cl atoms increases. This observation is significant because it shows a distortion of the all *trans*–*trans* zigzag conformation of the backbone at higher chlorine contents. Another region of particular interest is the  $700\text{--}850\text{ cm}^{-1}$  region where methylene rocking motions are observed. The resonance at  $758\text{ cm}^{-1}$  has been assigned to the methylene rocking motion in PVC, specifically the rocking mode of a  $\text{CH}_2$  unit between two  $\text{CHCl}$  units. As the concentration of  $\text{CH}_2$  units increases going from PVC through the EVC series, the peak at  $758\text{ cm}^{-1}$  decreases in intensity and the peak at  $723\text{--}718\text{ cm}^{-1}$  increases in intensity, which is characteristic of  $\text{CH}_2$  rocking modes for longer methylene sequences. In the case of PE a doublet is observed at  $730$  and  $719\text{ cm}^{-1}$ , which has been assigned to rocking vibrations of long methylene sequences. This doublet in PE, which is specifically associated with the orthorhombic crystal structure, is not observed for any of the EVC polymers suggesting that a different crystalline structure exists for these materials.<sup>38</sup>

Bands between  $1400$  and  $900\text{ cm}^{-1}$  are difficult to assign to individual vibrational components, since most resonances overlap with other resonances. The numerous resonances in this region are rapidly reduced in intensity as the number of chlorines is decreased. Exceptions are the  $1332$  and  $963\text{ cm}^{-1}$  bands, which are dominated by C–C stretching and  $\text{CH}_2$  wagging motions of short sequences. In the case of EVC polymers, the peak at  $1332\text{ cm}^{-1}$  decreases with decreasing chlorine content, and the peak at  $963\text{ cm}^{-1}$  fully disappears for all of the EVC polymers. Additionally, all the peaks in the area of the  $1254\text{ cm}^{-1}$  multiplet arise from methine bending modes and are sensitive to sequence length and/or environment. The decrease in the intensity of the  $1254\text{ cm}^{-1}$  peak with decreasing chlorine content is indicative of the smaller chlorine contents and the changing environment caused by the presence of longer methylene sequences.<sup>38</sup>

The C–H bending modes at  $1435/1426\text{ cm}^{-1}$  for PVC broaden into a singlet as the number of chlorines is decreased. Concomitant with the  $1435/1426\text{ cm}^{-1}$  loss is the growth of the  $1467\text{--}1471\text{ cm}^{-1}$  resonance which eventually becomes the  $1472/1462\text{ cm}^{-1}$  doublet assigned to the methylene bending modes in PE.<sup>38</sup> The shoulders observed in the EVC samples at  $1457$  and  $1434\text{ cm}^{-1}$  correspond to the bending modes for the  $\beta$  and  $\alpha$  methylenes. It can be observed that the intensity of the peaks at  $1457$  and  $1434\text{ cm}^{-1}$  increases with increasing chlorine content in the EVC polymers. The above IR study clearly

**Figure 2.** IR of PE, **PE21Cl**, **PE15Cl**, **PE9Cl**, and PVC.



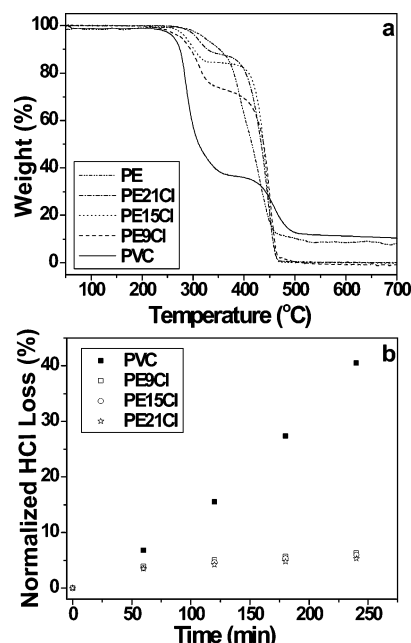


**Figure 3.** (a) TGA results for PE, PE21Cl, PE15Cl, PE9Cl, and PVC. (b) Normalized HCl loss data for PVC, PE9Cl, PE15Cl, PE21Cl under isothermal (180 °C) degradation measured under nitrogen atmosphere.

illustrates the evolution of the PVC structure through a series of precise EVC polymers with decreasing chlorine content to the pure PE backbone.

**Thermal Analysis: TGA.** While NMR and IR support the proposed primary structure, TGA results directly support the precise composition of the polymers. Figure 3a displays the thermal decomposition curves of all three polymers as shown relative to PE and PVC. All three EVC polymers exhibit a two-stage decomposition, where the first stage corresponds to the loss of HCl and the second stage marks the catastrophic decomposition of the polymer. Analogous to our previous work on ethylene vinyl halide polymers and the reported decomposition of PVC, the mass loss in the first stage quantitatively reflects the halogen content of the polymer. The observed values for mass loss in the first stage are found to be in agreement with the calculated HCl content for each of the EVC polymers at 23%, 15%, and 11% for PE9Cl, PE15Cl, and PE21Cl respectively. Figure 3a also shows that the onset of decomposition for the first stage loss of HCl increases with decreasing chlorine content (see Table 1). The EVC samples become more stable with increasing content of ethylene units as the labile chlorine content decreases, since the chain reaction (zipper mechanism) resulting in HCl loss is restricted by more ethylene units compared to PVC. This effect is called inner stabilization.<sup>13</sup> The stabilization of the EVC samples can also be partially attributed to the lack of tertiary or allylic chlorines, which are generally found in PVC. However in the second stage of decomposition, the onset for PVC is higher than that for the EVC polymers and this difference can be attributed to a high concentration of conjugated carbon–carbon double bonds that begin to cross-link and are converted into char.<sup>41</sup> Even at temperatures above 500 °C, after the EVC polymers have completely decomposed, residual char is observed in PVC and a nonzero mass is observed in PE, which is attributed to catalyst residue.

Figure 3b compares the stability of the EVC polymers to that of PVC under isothermal decomposition at 180 °C. Here, a temperature of 180 °C is chosen as it is below the onset of decomposition for any of the polymers, ensuring that any mass

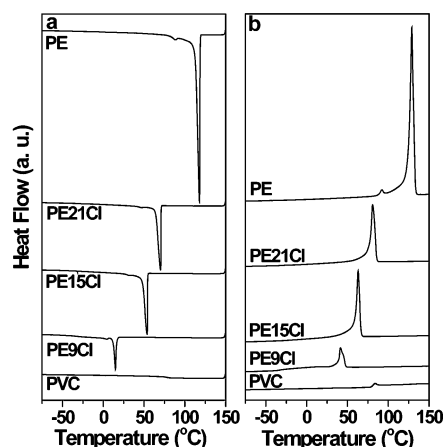


**Figure 4.** DSC exotherms (a) and endotherms (b) of PE9Cl, PE15Cl, PE21Cl, relative to PE and PVC.

loss may be attributed to HCl loss. The percentage HCl loss is normalized to the overall HCl content in each of the polymers to reflect the relative amount of a given polymer's HCl loss over a given time interval. All samples undergo a rapid loss of 3.5–6.8% of the total HCl content of the polymer during the first hour. However, after the first hour, the degradation rate of the EVC polymers levels off leading to a total HCl loss of only ~6% even after 4 h at 180 °C, while the PVC sample continues to degrade at nearly a constant rate, leading to the loss of ~40% of the HCl content after 4 h. Structural precision and the absence of defects make the difference. Precise EVC polymers are more stable to the applied isothermal decomposition than PVC, a result which can be attributed to the suppression of the zipper mechanism found in PVC and induced by the extended spacing between chlorine atoms (referred to as inner stabilization as described above) in the precise polymers.

**DSC.** The DSC data for the precision polymers is shown relative to that for PE and PVC in Figure 4 for both the crystallization (Figure 4a) and melting (Figure 4b) behavior, and the results are summarized in Table 1. Increasing the chlorine atom content results in a decrease of  $T_m$ , and  $\Delta H_m$ . This behavior indicates an increase in the degree of disorder in the crystal owing to the introduction of the chlorine atom into the crystal lattice. When we compare these results with our previous work on precision ethylene/vinyl bromide polymers,<sup>33</sup> it becomes clear that Br atoms lower the melting point and  $\Delta H_m$  more than the chlorine atoms for polymers with the same halogen content. Assuming a similar distribution of the halogen (Cl or Br) between crystalline and noncrystalline regions,<sup>32</sup> the difference in thermal behavior correlates with larger lattice strains in the precision vinyl bromide series.

The sharp crystalline and melting traces seen in Figure 4 are typical of homopolymers and are in stark contrast to the broad traces observed in random EVC polymers of similar chlorine content.<sup>19</sup> This suggests a difference in the crystallization process for ADMET EVC polymers relative to random EVC polymers, which is not based on the selection of long crystallizable sequences. It is likely that the crystallization of precisely substituted Cl samples evolves by incorporating in the crystallite long chain segments without chlorine discrimination.<sup>32</sup> PE9Cl displays a sharp crystallization peak and a dual melting transition, the latter caused by a melting–recrystallization process enabled by the presence of relatively high Cl contents in the crystal (see supporting documentation). The lower melting peak corresponds to the initial crystallites, while crystals formed during the heating scan melt at a higher temperature. Recrys-

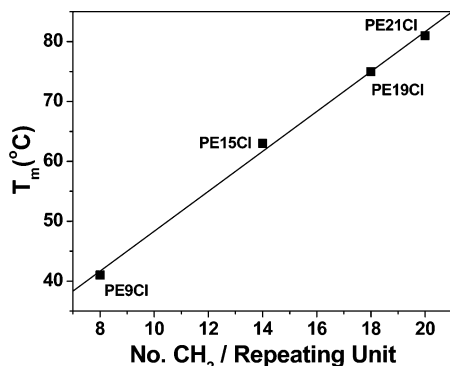


**Figure 5.** Trends for the variation in  $T_m$  vs the number of  $\text{CH}_2$  per repeat unit.

tallization is suppressed at the heating rate of 40 °C/min. Reducing the Cl content in the series, and hence in the crystal, leads to less defected, thicker crystallites not subject to melt-recrystallization as indicated in Figure 4 by sharp single meltings of **PE15Cl** and **PE21Cl**. The dramatic decrease of heat of fusion for **PE9Cl** relative to **PE15Cl** and **PE21Cl** suggests a lower degree of crystallinity, indicating that the increased content of bulky atoms along the chain inhibits the ability of the polymer to crystallize to a greater extent. The greater amorphous content of **PE9Cl** is evidenced by a more visible  $T_g$  relative to the other precise polymers. Interestingly we observe a linear correlation between the  $T_g$  of PVC at 80 °C, the  $T_g$  of PE at −120 °C,<sup>42</sup> and the value for **PE9Cl** at −33 °C with mass fraction of Cl in the polymer. The glass transition temperature of **PE9Cl** decreases with decreasing chlorine content relative to PVC due to the high mobility of the ethylene units.

Figure 5 shows the linear relationship between  $T_m$  and the number of  $\text{CH}_2$  groups in the repeating unit. In accord with the behavior of *trans*-poly(alkenamers), the melting temperature increases with increasing number of carbon atoms in the repeating unit for materials that crystallize with the same crystal structure, as is expected in this case.

**Conclusion and Outlook.** Herein we have described the synthesis of a family of precise ethylene/vinyl chloride polymers that contain a chlorine atom on each and every ninth, 15th, and 21st carbon respectively. The precise primary structure has been confirmed by  $^1\text{H}$  NMR and  $^{13}\text{C}$  NMR spectroscopy, which allow for the assignment of each chemical shift observed to one unique methylene or methine group within the repeat unit. The presence of only those shifts corresponding to a precision polymer reinforces the ability of ADMET to generate precise and defect free polymers. The thermal characterization of the polymers via DSC suggests a crystallization process typical of homopolymers as evidenced by the sharp melting and crystallization transitions. The homopolymer behavior is indicative of a precise structure that crystallizes in such a fashion to incorporate the chlorine atoms into the crystal lattice, in sharp contrast to random EVC polymers. Melting and crystallization temperatures scale proportionally to the number of  $\text{CH}_2$  groups in the repeating unit. The heat of fusion decreases drastically with increasing Cl content in the series, with values of <30 J/g for **PE9Cl** suggesting that beyond a certain critical chlorine content in these precise polymers, the bulky chlorine atoms begin to inhibit the crystallization process. Further work aimed to provide direct evidence of the crystal structure via WAXD, crystal composition via solid-state NMR and lamellar morphology is currently underway.

## Experimental

**Chemicals.** Chemicals were purchased from the Aldrich Chemical Co. and used as received unless noted. Grubbs' first generation ruthenium catalyst, bis(tricyclohexylphosphine)benzylidene ruthenium(IV)dichloride, was purchased from Strem Chemical and stored in an argon filled dry box prior to use. Methylene chloride and *o*-xylene were distilled over  $\text{CaH}_2$ . The same ADMET PE sample published<sup>34</sup> by our group was used for comparison. PVC was purchased from the Aldrich Chemical Co., Product Number 389293.

**Instrumentation.** Solution  $^1\text{H}$  NMR (300 MHz) and  $^{13}\text{C}$  NMR (75 MHz) spectra were recorded on a Varian Gemini 300, VXR 300 or Mercury 300 spectrometer. All chemical shifts for  $^1\text{H}$  and  $^{13}\text{C}$  NMR spectroscopy were referenced to residual signals from  $\text{CDCl}_3$  ( $^1\text{H}$  = 7.27 ppm and  $^{13}\text{C}$  = 77.23 ppm) with an internal reference TMS 0.03% v/v to internal TMS standard for 0. The **UPEXCl** polymers were also characterized by standard 2D NMR experiments run on a Varian Inova 500 instrument (500 MHz for  $^1\text{H}$  and 125 MHz for  $^{13}\text{C}$ ). In all the NMR work, the solvent was chloroform-*d* and the temperature was 25 °C.

High-resolution mass spectral (HRMS) data were obtained on a Finnegan 4500 gas chromatograph/mass spectrometer using the electron ionization (EI) mode. Elemental analyses were carried out by Atlantic Microlabs Inc., Norcross, GA. The GPC measurements for samples in THF were taken on a Waters GPCV 2K instrument. Samples were run with HPLC grade THF at 40 °C on Waters StyragelHR 5E columns monitored with an internal differential refractive index detector (DRI) relative to polystyrene standards. Polymer molecular weights reported vs polyethylene standards were measured using a Waters Associates 150C high-temperature gel permeation chromatograph equipped with three Polymer Laboratories mixed bed Type B columns and an internal DRI detector. The mobile phase was BHT-inhibited 1,2,4-trichlorobenzene (135 °C, flow rate 1.0 mL/minute, typical sample concentration 2 mg/mL). IR data was obtained using a Perkin-Elmer Spectrum One FTIR outfitted with a LiTaO<sub>3</sub> detector. Measurements were automatically corrected for water and carbon dioxide. Thermogravimetric analysis (TGA) data was obtained with a Perkin-Elmer 7 series thermal analysis system. The TGA samples (2–5 mg) were heated from 50 to 700 °C at 10 °C/min under nitrogen. Melting and crystallizations were obtained at 10 °C/min in a differential scanning calorimeter TA Instrument DSC-Q1000 V9.6 Build 290 under nitrogen flow and were calibrated with indium.

**Synthesis. General Procedure for Grignard Reaction.** Synthesis of 5-bromopent-1-ene (**1**), 8-bromooct-1-ene (**2**), 11-bromoundec-1-ene (**3**), undeca-1,10-dien-6-ol (**4**), heptadeca-1,16-dien-9-ol (**5**), and tricos-1,22-dien-12-ol (**6**) were described previously.<sup>32</sup>

**General Procedure for the Chlorination Reaction.** The precursor alcohol **4**, **5**, or **6** (1 equiv) and  $\text{Ph}_3\text{P}$  (1.5 equiv) were dissolved in  $\text{CCl}_4$  under argon. The reaction was stirred overnight at 80 °C. The solution was concentrated, and pentane was added. The mixture was filtered, and the filtrate was concentrated under vacuum to yield chlorinated ADMET monomer 6-chloroundeca-1,10-diene (**7**), 9-chloroheptadeca-1,16-diene (**8**), or 12-chlorotricos-1,22-diene (**9**), respectively. The chlorinated ADMET monomers were purified with column chromatography on silica gel eluted by hexane (yield 70–80%).

**6-Chloroundeca-1,10-diene (7).**  $^1\text{H}$  NMR (300 MHz  $\text{CDCl}_3$ ):  $\delta$  5.81 (m, 2H), 5.00 (m, 4H), 3.91 (p, 1H), 2.09 (m, 4H), 1.81–1.42 (br, 8H).  $^{13}\text{C}$  NMR (75 MHz,  $\text{CDCl}_3$ ):  $\delta$  138.55, 115.09, 64.00, 38.08, 33.40, 25.90. HRMS: calcd for  $\text{C}_{11}\text{H}_{19}\text{Cl}$  ( $\text{M} + \text{Cl}$ )<sup>+</sup>, 221.0858; found, 221.0866. Anal. Calcd for  $\text{C}_{11}\text{H}_{19}\text{Cl}$ : C, 70.76; H, 10.26; Cl, 18.99. Found: C, 70.93; H, 10.25; Cl, 18.74.

**9-Chloroheptadeca-1,16-diene (8).**  $^1\text{H}$  NMR (300 MHz  $\text{CDCl}_3$ ):  $\delta$  5.81 (m, 2H), 4.97 (m, 4H), 3.90 (p, 1H), 2.05 (m, 4H), 1.70 (m, 4H), 1.60–1.20 (br, 16H).  $^{13}\text{C}$  NMR (75 MHz,  $\text{CDCl}_3$ ):  $\delta$  139.31, 114.44, 64.52, 38.71, 33.96, 29.24, 29.19, 29.04, 26.66. HRMS: calcd for  $\text{C}_{17}\text{H}_{31}\text{Cl}$  ( $\text{M}^+$ ), 270.2114; found, 270.2112. Anal. Calcd for  $\text{C}_{17}\text{H}_{31}\text{Cl}$ : C, 75.38; H, 11.54; Cl, 13.09. Found: C, 75.53; H, 11.52; Cl, 13.00.

**12-Chlorotricosa-1,22-diene (9).**  $^1\text{H}$  NMR (300 MHz  $\text{CDCl}_3$ ):  $\delta$  5.81 (m, 2H), 4.97 (m, 4H), 3.89 (p, 1H), 2.04 (m, 4H), 1.71 (m, 4H), 1.60–1.20 (br, 28H).  $^{13}\text{C}$  NMR (75 MHz,  $\text{CDCl}_3$ ):  $\delta$  139.45, 114.33, 64.61, 38.75, 34.03, 29.73, 29.72, 29.68, 29.41, 29.35, 29.16, 26.72. HRMS: calcd for  $\text{C}_{23}\text{H}_{43}\text{Cl}$  ( $\text{M}^+$ ), 354.3053; found, 354.3066. Anal. Calcd for  $\text{C}_{23}\text{H}_{43}\text{Cl}$ : C, 77.81; H, 12.21; Cl, 9.99. Found: C, 77.88; H, 12.22; Cl, 10.00.

**General Procedure for Bulk Polymerization.** Monomer and Grubbs' first generation catalyst were combined in a ratio of 500:1 under argon atmosphere. The polymerization was conducted at 35–40 °C under vacuum with stirring for 5 days. The reaction was then stopped and 5 mL of toluene was added to dissolve the polymer with stirring. The reaction was allowed to cool to room temperature. The polymers were then precipitated by dripping the toluene solution into cold acidic methanol. They were then isolated by filtration and dried. Polymers were then redissolved in 50 mL of toluene and treated with THP (tris(hydroxymethyl)phosphine) in order to remove any residual catalyst.<sup>43</sup> The polymers were then reprecipitated into acidic methanol, filtered, and dried.

**Polymerization of 6-Chloroundeca-1,10-diene (UPE9Cl).**  $M_w$  (GPC vs PS) = 37 100 g/mol. PDI = ( $M_w/M_n$ ) = 1.84. For  $^1\text{H}$  NMR and  $^{13}\text{C}$  NMR data, see Table 2.

**Polymerization of 9-Chloroheptadeca-1,16-diene (UPE15Cl).**  $M_w$  (GPC vs PS) = 39 800 g/mol. PDI = ( $M_w/M_n$ ) = 1.81. For  $^1\text{H}$  NMR and  $^{13}\text{C}$  NMR data, see Table 2.

**Polymerization of 12-Chlorotricosa-1,22-diene (UPE21Cl).**  $M_w$  (GPC vs PS) = 67 100 g/mol. PDI = ( $M_w/M_n$ ) = 1.84. For  $^1\text{H}$  NMR and  $^{13}\text{C}$  NMR data, see Table 2.

**General Procedure for Hydrogenation.** The chlorine containing polymers (UPE9Cl, UPE15Cl, and UPE21Cl) were then hydrogenated using a modified version of the method described by Hahn<sup>33</sup> by dissolving in dry *o*-xylene under argon and adding 3.3 equiv of *p*-toluenesulfonyl hydrazide (TSH) and 4 equiv of tri-*n*-propyl amine (TPA). The solutions were refluxed for 9 h and then cooled to room temperature. The hydrogenated polymer was precipitated into ice-cold methanol and isolated by filtration. The dried polymer was then redissolved in toluene and reprecipitated by dipping into ice-cold acidic methanol. A white solid was collected by filtration and the polymers were isolated in quantitative yield.

**PE9Cl.**  $^1\text{H}$  NMR (300 MHz  $\text{CDCl}_3$ ):  $\delta$  3.89 (p, 1H), 1.71 (m, 4H), 1.62–1.0 (bm, 12H).  $^{13}\text{C}$  NMR (75 MHz,  $\text{CDCl}_3$ ):  $\delta$  64.58, 38.75, 29.64, 29.37, 26.71. Anal. Calcd: C, 67.27; H, 10.66; Cl, 22.06. Found: C, 67.25; H, 10.65; Cl, 20.92.  $M_w$  (GPC vs PS) = 48 700 g/mol. PDI = ( $M_w/M_n$ ) = 1.78.

**PE15Cl.**  $^1\text{H}$  NMR (300 MHz  $\text{CDCl}_3$ ):  $\delta$  3.90 (p, 1H), 1.71 (m, 4H), 1.6–1.2 (bm, 24H).  $^{13}\text{C}$  NMR (75 MHz,  $\text{CDCl}_3$ ):  $\delta$  64.63, 38.76, 29.90, 29.87, 29.82, 29.76, 29.43, 26.74. Anal. Calcd: C, 73.58; H, 11.94; Cl, 14.48. Found: C, 73.66; H, 12.00; Cl, 14.26.  $M_w$  (GPC vs PS) = 51 400 g/mol. PDI = ( $M_w/M_n$ ) = 1.75.

**PE21Cl.**  $^1\text{H}$  NMR (300 MHz  $\text{CDCl}_3$ ):  $\delta$  3.90 (p, 1H), 1.74 (m, 4H), 1.6–1.2 (bm, 36H), 0.9 (t, 0.15H).  $^{13}\text{C}$  NMR (75 MHz,  $\text{CDCl}_3$ ):  $\delta$  64.62, 38.76, 29.94, 29.88, 29.82, 29.76, 29.44, 26.74. Anal. Calcd: C, 76.66; H, 12.56; Cl, 10.78. Found: C, 76.64; H, 12.61; Cl, 10.57.  $M_w$  (GPC vs PE) = 31 100 g/mol. PDI = ( $M_w/M_n$ ) = 4.43.

**Acknowledgment.** Funding of this work by the National Science Foundation, Grants NSF 314110 and DMR-0503876, is gratefully acknowledged. Generous support from ARO for the acquisition of catalysts is also acknowledged. We also gratefully acknowledge Dr. Lisa Baugh at Exxon-Mobil for obtaining high-temperature GPC data for PE21Cl.

**Supporting Information Available:** Figure S1, DSC endotherms for PE9Cl at heating rates of 5, 10, and 40 °C/min. This material is available free of charge via the Internet at <http://pubs.acs.org>.

## References and Notes

- Braun, D. *J. Vinyl Addit. Technol.* **2001**, *7*, 168–176.
- Smalley, D. In *PVC Handbook*; Wilkes, C. E., Summers, J. W., Daniels, C. A., Eds.; Hanser: Munich, 2005; pp 679–700.
- Allsopp, M. W.; Vianello, G. In *Encyclopedia of Polymer Science and Technology*; Kroschwitz, J. I., Ed.; Wiley: New Jersey, 2003; Vol. 8, pp 437–476.
- Witenhafer, D. E.; Poledna, D. J. In *PVC Handbook*; Wilkes, C. E., Summers, J. W., Daniels, C. A., Eds.; Hanser: Munich, 2005; pp 57–94.
- Matthews, G. *PVC: Production, Properties, and Uses*; The Institute of Materials: London, 1996; pp 41–62.
- Kline, M. W.; Skiest, E. N. In *Encyclopedia of PVC*; Nass, L. I., Ed.; Marcel Dekker: New York, 1976; pp 109–175.
- Kline, M. W.; Skiest, E. N. In *Encyclopedia of PVC*; Nass, L. I., Ed.; Marcel Dekker: New York, 1976; pp 138–139.
- Wilkes, C. E.; Westfahl, J. C.; Backderf, R. H. *J. Polym. Sci.: Part A-1* **1969**, *7*, 23–33.
- Hagiwara, M.; Miura, T.; Kagiya, T. *J. Polym. Sci.: Part A-1* **1969**, *7*, 513–523.
- Boone, H. W.; Athey, P. S.; Mullins, M. J.; Philipp, D.; Muller, R.; Goddard, W. A. *J. Am. Chem. Soc.* **2002**, *124*, 8790–8791.
- Boffa, L. S.; Novak, B. M. *Chem. Rev.* **2000**, *100*, 1479–1493.
- Jameison, F. A.; Schilling, F. C.; Tonelli, A. E. *Macromolecules* **1986**, *19*, 2168–2173.
- Braun, D.; Mao, W.; Bohringer, B.; Garbella, R. W. *Die Angew. Makromol. Chem.* **1986**, *141*, 113–129.
- Pourahmady, N.; Bak, P. I.; Kinsey, R. A. *J. Macromol. Sci. Pure Appl. Chem.* **1992**, *29*, 959–974.
- Stoeva, S.; Vlaev, L. *Macromol. Chem. Phys.* **2002**, *203*, 346–353.
- Chang, B. H.; Zeigler, R.; Hiltner, A. *Polym. Eng. Sci.* **1988**, *28*, 1167–1172.
- Era, V. A. *Makromol. Chem.* **1974**, *175*, 2191–2198.
- Friese, K.; Hobelbarth, B.; Reinhardt, J.; Neue, R. *Angew. Makromol. Chem.* **1996**, *234*, 119–132.
- Bowmer, T. N.; Tonelli, A. E. *Polymer* **1985**, *26*, 1195–1201.
- Gomez, M. A.; Tonelli, A. E.; Lovinger, A. J.; Schilling, F. C.; Cozine, M. H.; Davis, D. D. *Macromolecules* **1989**, *22*, 4441–4451.
- Cais, R. E.; Kometani, J. M. *Macromolecules* **1982**, *15*, 954–960.
- Sobotka, J. *Acta Polym.* **1983**, *34*, 647–650.
- Zhikuan, C.; Lianghe, S.; Sheppard, R. N. *Polymer* **1984**, *25*, 369–374.
- Saito, T.; Matsumura, Y.; Hayashi, S. *Polym. J.* **1970**, *1*, 639–655.
- Chang, B. H.; Dai, J. W.; Siegmund, A.; Hiltner, A. *Polym. Eng. Sci.* **1988**, *28*, 1173–1181.
- Gutzler, F.; Wegner, G. *Colloid Polym. Sci.* **1980**, *258*, 776–786.
- Hanna, R. J.; Fields, J. W. *J. Vinyl Technol.* **1982**, *4*, 57–61.
- Stephens, C. H.; Yang, H.; Islam, M.; Chum, S. P.; Rowan, S. J.; Hiltner, A.; Baer, E. *J. Polym. Sci., Part B: Polym. Phys.* **2003**, *41*, 2062–2070.
- Lopez, D.; Reinecke, H.; Hidalgo, M.; Mijangos, C. *Polym. Int.* **1997**, *44*, 1–10.
- Baughman, T. W.; Wagener, K. B. *Adv. Polym. Sci.* **2005**, *176*, 1–42.
- Yang, H.; Islam, M.; Budde, C.; Rowan, S. J. *J. Polym. Sci., Part A: Polym. Chem.* **2003**, *41*, 2107–2116.
- Boz, E.; Wagener, K. B.; Ghosal, A.; Fu, R.; Alamo, R. G. *Macromolecules* **2006**, *39*, 4437–4447.
- Boz, E.; Nemeth, A. J.; Alamo, R. G.; Wagener, K. B. *Adv. Synth. Catal.* **2007**, *349*, 137–141.
- Hahn, S. F. *J. Polym. Sci., Part A: Polym. Chem.* **1992**, *30*, 397–408.
- Sworen, J. C.; Smith, J. A.; Wagener, K. B.; Baugh, L. S.; Rucker, S. P. *J. Am. Chem. Soc.* **2003**, *125*, 2228–2240.
- Brandrup, J.; Immergut, E. H.; Grulke, E. A. *Polymer Handbook*, 4th ed.; Wiley-Interscience, New York, 1984.
- Schilling, F. C.; Tonelli, A. E.; Valenciano, M. *Macromolecules* **1985**, *18*, 356–360.
- Wu, T. K. *Macromolecules* **1973**, *6*, 737–741.
- Bowmer, T. N.; Tonelli, A. E. *J. Polym. Sci., Part B: Polym. Phys.* **1986**, *24*, 1631–1650.
- Stoeva, S. *J. Appl. Polym. Sci.* **2004**, *94*, 189–196.
- Vogl, O.; Qin, M. F.; Zilkha, A. *Prog. Polym. Sci.* **1999**, *24*, 1481–1525.
- Stehling, F. C.; Mandelkern, L. *Macromolecules* **1970**, *3*, 242–252.
- Maynard, H. D.; Grubbs, R. H. *Tetrahedron Lett.* **1999**, *40*, 4137–4140.